Undersea Biomedical Research, Vol. 14, No. 3, May 1987

Components of the pressure required to breathe dense gases

H. D. VAN LIEW

Department of Physiology, State University of New York at Buffalo, Buffalo, NY, 14214

Van Liew HD. Components of the pressure required to breathe dense gases. Undersea Biomed Res 1987; 14(3):263–276.—To elucidate the impact of high gas density on airway flow (during inspiration and expiration) and on gas acceleration (at end-inspiration and end-expiration), I simulated pressures for breathing in man with a) an equation of motion of the respiratory system, b) the assumption that pressure to accelerate gas is directly proportional to density, and c) five different assumptions concerning the relationships among lung volume, density, and the pressure for flow. The results show that accelerative pressure is not an important fraction of the total pressure with attainable densities, tidal volumes, and frequencies when it is assumed that lung volume changes as a sine-wave function of time. High accelerative pressure has a minor effect of making intrapleural pressure tend to be in phase with flow, as it is with high flow resistance. Alternate assumptions about pressure to cause flow led to small changes in the patterns of pressure with time, but had little effect on the overall picture. Conclusions: Effects of lung volume and density on flow pressure can be characterized successfully in several ways, and the large density effect on flow pressure dominates the energy requirement for breathing in dense-gas environments.

airways
density-dependence of resistance
elastic recoil
gas density
hyperbaric
volume-dependence of resistance
inertance
natural frequency of the respiratory system
pulmonary resistance
resonant frequency
Rohrer equation

How will breathing of dense gas, as in a hyperbaric environment, change the pressures that must be generated by a person's respiratory musculature? One of the goals of this communication is to explore the consequences of changes of gas density and breathing pattern on the pulmonary mechanical system. The approach is to simulate the pressures for ventilating a simple, one-compartment human lung using the commonly accepted general assumption that the mechanical system can be characterized in terms of a resistance, a compliance, and an inertance.

One necessary specific assumption is how pressure for accelerating gas is related to gas density. Inertance of the human respiratory system is negligible in a normal air environment, but has been shown experimentally to increase in direct proportion

to density of the breathing gas (1–3); a practical question is whether the entity that has been called "volume acceleration" (4) can become as important as resistance and compliance in very dense environments.

A second specific assumption, or set of assumptions, involves the interrelationships among pressure, flow, lung volume and gas density; inasmuch as several different approaches to these interrelationships have been put forward in the past, this communication includes simulations with different sets. A second goal of the communication is to provide perspective on the different assumptions. Does choice of assumption set make a substantive difference to the outcome of the calculations?

Pressure-flow assumptions

The pressure-flow relationship for gases is more complicated than the implication, by analogy with an electrical system, that voltage (pressure) and current (flow) should be simply proportional to each other, so I shall hereafter eschew the term "resistance" altogether in favor of "ratio of flow pressure to flow." In 1915 Rohrer (5) introduced a scheme for dealing with the complication; pressure for flow (P_{flow}) was related to flow [the first derivative of volume (V) with respect to time (t)] and the square of flow by two constants, K_1 and K_2:

$$P_{flow} = K_1\, dV/dt + K_2\, (dV/dt)^2.$$

One alternative to the Rohrer formulation was presented by Maio and Farhi (6) in a study of men who hyperventilated while breathing gases of various densities; the data fit an empirical formula in which pressure was proportional to a single term containing flow raised to the power 1.6. Data for mouth occlusion pressure ($P_{0.1}$, an index of respiratory drive, and thus an indirect index of flow pressure) from men exercising in a hyperbaric environment (7) support the Maio-Farhi approach; $P_{0.1}$ increased in proportion to average inspiratory flow raised to the power 1.4.

The role of density in the pressure-flow relationship is debatable; it is presumably related to inertial effects on convective acceleration and other phenomena. Some authors suggest that the density dependence of flow pressure should reside in the Rohrer K_2 term (8). In contrast, Pedley et al. (9) gave theoretical reasons why pressure for flow should increase as the square root of density; they put forward the formulation

$$P_{flow} = K^p\, (\, RGD\, u\,)^{0.5}\, (dV/dt)^{1.5}$$

where K_p is a coefficient that presumably depends on lung anatomy and u is viscosity of the gas. For some of my simulations, I chose to put this formulation into the context of the Rohrer equation by assuming that both the Rohrer terms should be multiplied by the square root of relative gas density (RGD). Data for exercising men reported by Wood and Bryan (10) show that submaximal flows at a given pressure are inversely proportional to the square root of RGD, and $P_{0.1}$ was found to be proportional to $RGD^{0.5}$ (7). A complicating issue is that the pressure for flow depends on lung volume (11, 12).

Calculations

Definitions of variables, values of constants, and equations that embody the assumptions for the simulations are in Table 1; the primary assumption is Eq. *2*, the

TABLE 1
DEFINITIONS, CONSTANTS, AND EQUATIONS.

Definitions, units, and values of constants

a1 = volume-dependence coefficient of Eq. *9*, (liter/s)/cmH_2O = 1.116 [from (11)]

a2 = volume-dependence coefficient of Eq. *10*, (liter/s)^2/cmH_2O = 4.57 [from (11)]

b1 = volume-dependence constant of Eq. *9*, (liter/sec)/cmH_2O = 0.059 [from (11)]

b2 = volume-dependence constant of Eq. *10*, (liter/s)^2/cmH_2O = 0.563 [from (11)]

c1 = coefficient of Eq. *16*, cmH_2O/(liter/s) = 0.45 [from (6)]

c2 = constant of Eq. *16*, dimensionless = 0.63 [from (6)]

c3 = exponent of flow of Eq. *16*, dimensionless = 1.6 [from (6)]

C_{chest} = compliance of the chest, liter/cmH_2O

C_{lung} = compliance of the lung, liter/cmH_2O = 0.2 [from (13)]

C_{total} = compliance of the total respiratory system, liter/cmH_2O = 0.1 [from (13)]

f = breathing frequency, breaths/s

FRC = functional residual capacity, liters = 3

I_D = inertance in a dense environment, cmH_2O/(liter/s^2)

I_N = inertance in a normal environment, cmH_2O/(liter/s^2) = 0.01 [from (13)]

K_1 = first coefficient of the Rohrer equation, cmH_2O/(liter/s) = 1.2 [from (13)]

$K_{1'}$ = volume-dependent first coefficient of the Rohrer equation, cmH_2O/(liter/s), (derived by Eq. *9*)

K_{2D} = volume-independent second coefficient of the Rohrer equation in a dense environment, cmH_2O/(liter/s)^2

$K_{2D'}$ = volume-dependent second coefficient of the Rohrer equation in a dense environment, cmH_2O/(liter/s)^2 (derived by Eq. *11*)

K_{2N} = volume-independent second coefficient of the Rohrer equation in a normal environment, cmH_2O/(liter/s)^2 = 0.28 [from (13)]

$K_{2N'}$ = volume-dependent second coefficient of the Rohrer equation in a normal environment, cmH_2O/(liter/s)^2 (derived by Eq. *10*)

P_{accel} = pressure for accelerating and decelerating gas and tissue, cmH_2O

P_{chest} = pressure for overcoming elastic recoil of the chest and thorax, cmH_2O

P_{elast} = pressure for overcoming the elastic recoil of the respiratory system, cmH_2O

P_{flow} = pressure for causing flow, cmH_2O

P_{IPL} = intrapleural pressure, cmH_2O

PK_1 = pressure accounted for by the first term of the Rohrer equation (Eq. *8*), cmH_2O

TABLE 1 (continued)

P_{K_2}	=	pressure accounted for by the second term of the Rohrer equation (Eq. *8*), cmH_2O
P_{lung}	=	pressure for overcoming elastic recoil of the lung, cmH_2O
PNE	=	nonelastic pressure, cmH_2O
P_{total}	=	total pressure for breathing, cmH_2O
R	=	the ratio of flow pressure to flow, cmH_2O/(liter/s)
RGD	=	density in the dense environment as multiple of normal density dimensionless
t	=	time, s
TLC	=	total lung capacity, liters = 6
V	=	lung volume above FRC, liters
VC	=	vital capacity, liters = 5

Equations for general simulations—flow pressure is governed by a Rohrer equation having volume dependence; density dependence is located in the K_2 term.

$$V = \sin(2\pi f t) \quad (1)$$

$$P_{total} = P_{elast} + P_{flow} + P_{accel} \quad (2)$$

$$P_{elast} = P_{lung} + P_{chest} = V/C_{total} = (V + FRC)(1/C_{lung} + 1/C_{chest}) \quad (3)$$

$$P_{accel} = I_D\, d^2V/dt^2 \quad (4)$$

$$I_D = I_N\, RGD \quad (5)$$

$$R = P_{flow}/(dV/dt) \quad (6)$$

$$PNE = P_{total} - P_{elast} = P_{flow} + P_{accel} \quad (7)$$

$$P_{flow} = P_{K_1} + P_{K_2} = K_{1'}\, dV/dt + K_{2D'}\, (dV/dt)^2 \quad (8)$$

$$1/K_{1'} = b1 + a1\,(V+FRC)/TLC \quad (9)$$

$$1/K_{2N'} = b2 + a2\,(V+FRC)/TLC \quad (10)$$

$$K_{2D'} = K_{2N'}\, RGD \quad (11)$$

Optional equations—substituted for some of the equations above

$$P_{flow} = RGD^{0.5}\,(K_{1'}\, dV/dt + K_{2N'}\, (dV/dt)^2) \quad (12)$$

$$P_{flow} = RGD^{0.5}\,(K_1\, dV/dt + K_2\, (dV/dt)^2) \quad (13)$$

$$P_{flow} = K_1\, dV/dt + K_{2D}\, (dV/dt)^2 \quad (14)$$

$$K_{2D} = K_{2N}\, RGD \quad (15)$$

$$PNE = c1\,(RGD + c2)\, dV/dt^{c3} \quad (16)$$

equation of motion of the respiratory system as formulated by Mead (4). Calculations were simplified by use of Eq. *1*, the assumption that lung volume changes as a sine-wave function of time. Most values for constants came from the paper of Goldstein

and Mead (13). Equations *1–11* embody assumptions that were used for most simulations; I derived the a1, a2, b1, b2 constants used in Eqs. *9* and *10* from the K_1 and K_2 data for constant volumes reported by Bouhuys and Jonson (11), on the assumption that gas-flow conductance is a straight-line function of lung volume (12).

For certain simulations that are specified in the results section, various options embodied in Eqs. *12–15* for density dependence and volume dependence of the Rohrer equation were substituted for some of the lower-numbered equations. Volume dependence is implicit in Eq. *16* because of the way coefficients were derived from experimental data in which lung volume varied (6). The program for the simulations was written in Microsoft Basic.

RESULTS

Figure 1 illustrates the components of total pressure for 1-liter tidal volumes in a normal environment when frequency is 1/s. The *top panel* shows change of lung volume as a function of time; pressures to achieve this tidal volume are in the *lower panels*. Pressure to overcome elastic recoil (P_{elast}) is in phase with volume, pressure for flow (P_{flow}) is in phase with change of volume, and pressure for acceleration (P_{accel}) is ¼ cycle out of phase with flow, and therefore ½ cycle out of phase with volume and elastic recoil pressure *(second panel)*. Magnitude of the accelerative pressure is so small for this particular case that it is hardly visible on the diagram. Because P_{total} *(broken)* is the sum of the others, its peak occurs between the peaks for the two significant components, P_{elast} and P_{flow}. Negative P_{total} occurred toward the end of expiration—elastic recoil assisted expiration, but was not great enough to achieve the flow mandated by the 1-liter tidal volume and 1/s frequency. The P_{elast} *(third panel)* is comprised of pressure due to lung recoil (P_{lung}), which is always tending to deflate the thorax, and pressure due to chest recoil (P_{chest}), which approaches zero at end-inspiration as the chest nears its resting position.

For the Fig. 1 simulations, pressure for flow was calculated with a form of the Rohrer equation which embodies volume dependence. The *fourth panel* shows the two Rohrer equation components of P_{flow}, labeled PK_1 and PK_2. The PK_2 is about 30% smaller than PK_1 and because it increases as the square of flow, its trace has a sharper peak than a sine wave, making the P_{flow} pattern sharp also. The *lowest panel* shows the ratio of flow pressure to flow; the ratio shows the strong influence of flow and lesser influence of lung volume. The lowest minimum occurs when lung volume is greatest.

Figure 2 shows the pressure components for breaths in which pressure for acceleration is of consequence; assumptions are the same as in Fig. 1, and density dependence is accounted for by making K_2 of the Rohrer equation proportional to RGD. The format displays P_{total} and its components P_{elast}, P_{flow}, and P_{accel}, as in the *second panel* of Fig. 1 except that the contribution of PK_2 is plotted above that of PK_1. In the *upper left panel,* tidal volume is the same as in Fig. 1 but frequency is 6 times higher. The swings of P_{accel} are equal to swings of P_{elast}, so the system is by definition at its natural frequency, or resonant frequency. Because P_{elast} and P_{accel} counter each other, the P_{total} is almost completely due to P_{accel} and is in phase with flow. Note however that the very high pressures required for this 1-liter breath at such a high frequency make it an unrealistic case.

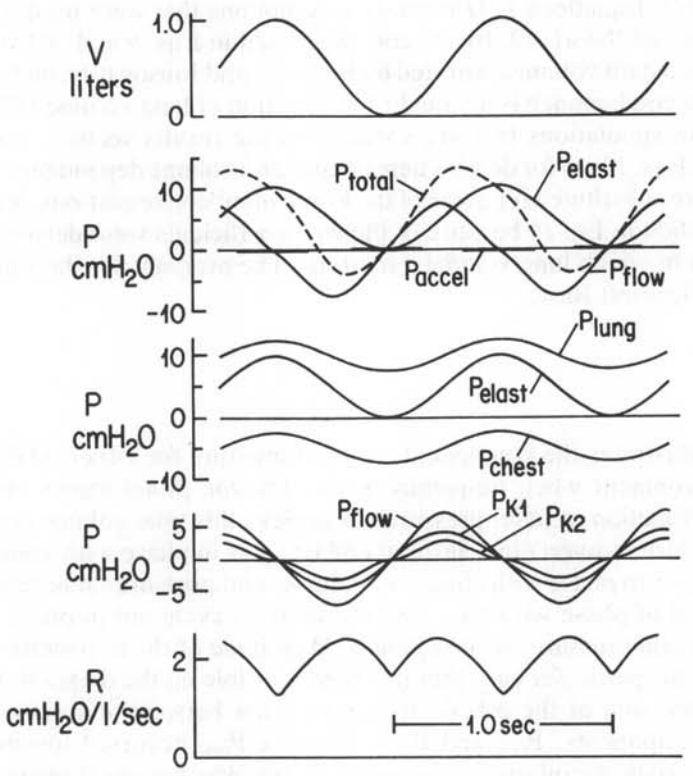

Fig. 1. Components of pressure for breathing normal air—1-liter tidal volumes at 1/s calculated with Eqs. *1–11* (Table 1). Note that the convention in all but one of the figures *(lower left,* Fig. 3) will be to plot pressure for breathing as if it were being applied by a pump ventilator, so a positive pressure is an inflating pressure. *Top panel,* lung volume above FRC. *Second panel,* total pressure *(broken),* pressure to overcome elastic recoil, pressure for flow, and pressure for acceleration of gas. *Third panel,* pressures due to lung recoil and chest recoil. *Fourth panel,* pressures for the first and second terms of the Rohrer equation (P_{K_1} and P_{K_2}), both referenced to the baseline; sum of the two is P_{flow}. *Bottom panel,* ratio of flow pressure-to-flow.

The *lower left panel* shows an attainable situation—the same high frequency as the panel above it but with a tidal volume of only 10 ml; this simulates the small-volume, high-frequency oscillations of the lung used in studies of lung impedance (14–19). The system is still at the natural frequency but the pressures involved are much less than in the panel above. The P_{flow} now has a negligible P_{K_2} component, so estimates of pressure-to-flow ratio from this breath would be due almost exclusively to the K_1 term of the Rohrer equation.

The *upper right panel* simulates high-frequency, 1-liter breaths when RGD = 10, as in air at 10 ATA. The total pressure to attain this pattern is again very large. The high density decreases the natural frequency; it is now 2/s, the frequency used for the simulation.

The case in the *lower right panel* simulates a small-sized tidal volume at RGD of 10 at the same high frequency of the two *left panels*. The P_{accel} *(oblique hatching)* is now greater than P_{elast}; the system is above its natural frequency. However the peak

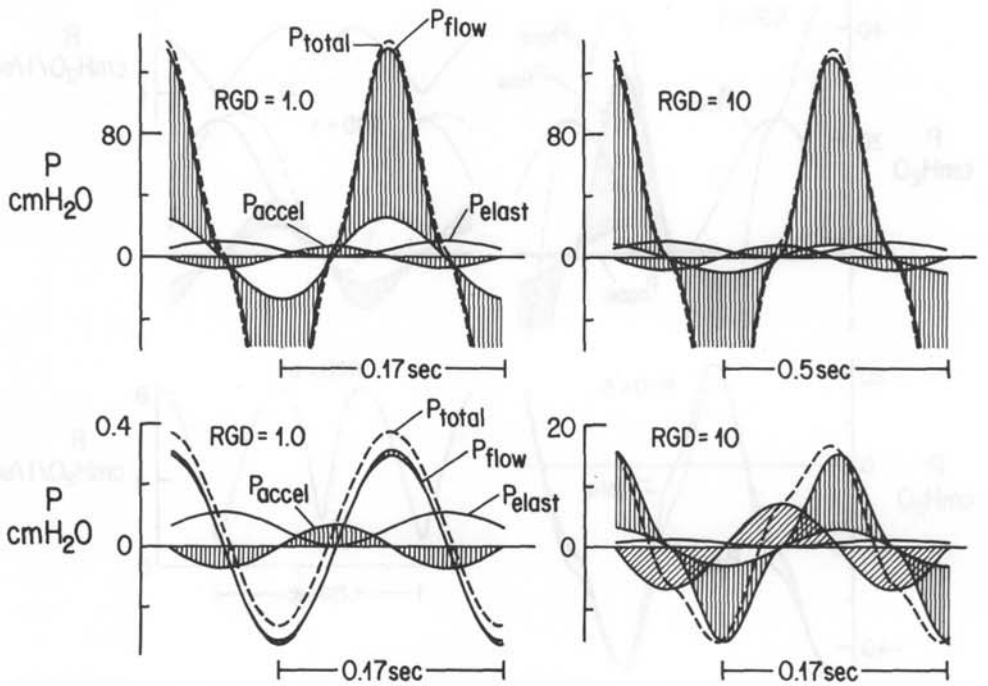

Fig. 2. Four cases in which pressure for acceleration is an important fraction of total pressure, simulated with Eqs. *1–11*. *Left panels,* normal gas density. *Right panels,* gas density is 10-fold normal. *Upper left,* 1-liter breaths at 6/s. *Lower left,* 10-ml breaths at 6/s. *Upper right,* 1-liter breaths at 2/s. *Lower right,* 100-ml breaths at 6/s. Contribution of P_{K_2} is *hatched* and plotted above or below contribution of P_{K_1} so that the vertical distance from the baseline to the sum of the two together is P_{flow}. The P_{accel} is also *hatched* for emphasis. In this and following figures, extremes of the pressure swings are sometimes truncated.

P_{total} is not much greater than P_{flow} since the P_{accel} contribution occurs out of phase with the P_{flow} contribution, and P_{flow} is still larger than P_{accel}.

Figure 3 shows simulations, using the same assumptions as in Figs. 1 and 2, of a real situation studied by Hesser et al. (20); men did maximal exercise while breathing air at 6 ATA. Elastic and flow pressures are about the same magnitude; accelerative pressure is negligible in comparison *(upper left)*. The simulated intrapleural pressure *(lower left)* is less than total pressure by the magnitude of the chest recoil pressure. The ratio of flow pressure-to-flow *(lower right)* varies between 1 and 8 $cmH_2O/(liter/s)$.

In simulations with normal gas density for the same tidal volume and frequency *(upper right quadrant,* Fig. 3), elastic recoil for the stated tidal volume is, of course, the same as in the dense environment, but pressure for flow is much less because the K_2 part of the flow pressure is reduced due to the lower density. Total pressure is due mainly to elastic recoil, but the total pressure curve is slightly nonsinusoidal because of the nonsinusoidal nature of the P_{K_2} contribution to the flow pressure, and ratio of flow pressure to flow varies between 1 and 2.5 $cmH_2O/(liter/s)$.

The *upper left panel* of Fig. 4 duplicates the *upper left panel* of Fig. 3; it has a large P_{K_2} caused by the K_2 being proportional to density. The other panels in Fig. 4 show calculations for the same tidal volume and frequency, but using various options for the dependences of flow pressure on lung volume and gas density—all but the case

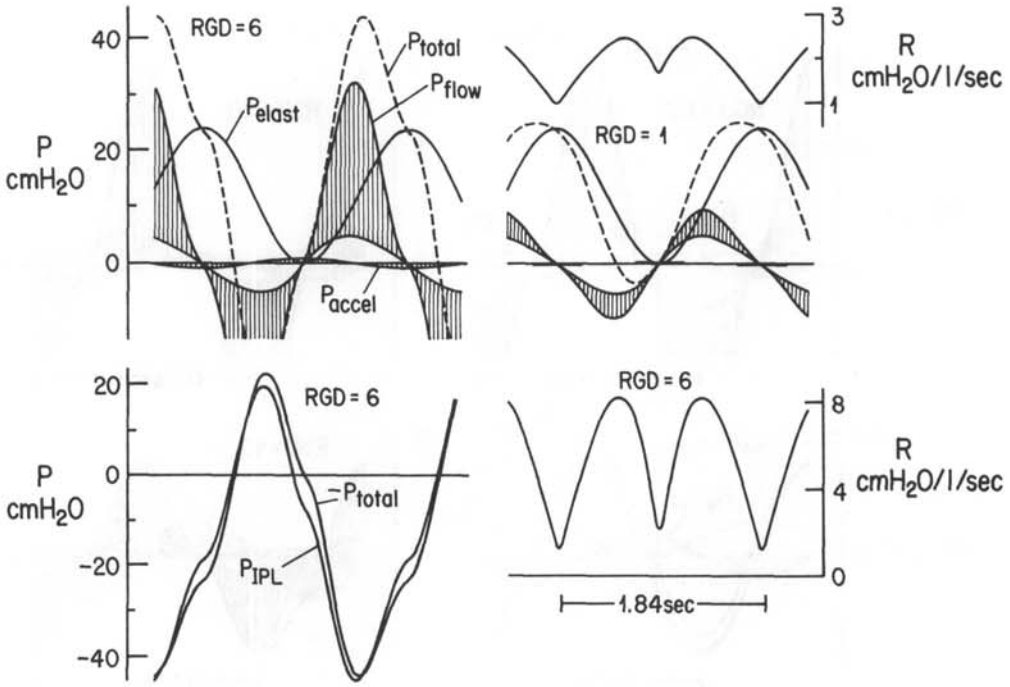

Fig. 3. Simulations, using Eqs. *1–11*, for a realistic case of exercising men; tidal volume = 2.43 liters at 0.54/s. *Left* and *lower right*, breathing air at 6 ATA. *Upper right quadrant*, same breaths at normal density. Variables are as in Figs. 1 and 2 except for the *lower left panel*, which shows intrapleural pressure and the negative of the P_{total}, for the case that the person, rather than a pump, generates pressure for the breath.

depicted in the *lower right panel* used the Rohrer equation. In the *upper middle panel*, volume dependence is the same as in the *upper left* and preceding figures; the changed assumption, that both K_1 and K_2 terms vary in proportion to the square root of gas density, caused the P_{K_2} component to diminish and the P_{total} to be less peaked. Absolute height of P_{total} is less, but this is not of particular interest; adjustment of coefficients could bring the height to the same level as in the upper left case. For the case shown at *lower left*, it was assumed that K_1 and K_2 had no volume dependence but that both varied with the square root of density as in the upper middle case; the result is intermediate between the previous two. In the *lower middle case*, it was assumed that there was no volume dependence but that all density dependence resided with K_2; the result is very similar to the upper left case. Finally, the *lower right panel* shows results of assuming the Eq. *16* relation between PNE, density, and flow with implicit volume dependence (6); P_{flow} and P_{total} resemble traces for the other cases.

Figure 5 shows nonelastic pressure (the sum of P_{flow} and P_{accel}) vs. flow for the various options depicted in Fig. 4. The relation of flow to time, mandated by the tidal volume and frequency, is the same for all traces in the figure, but pressures vary in magnitude and timing. The top two cases, having volume-dependent K_1 and K_2, form figure-of-eight patterns with relatively wide loops and with a crossover of the pressure near, but not at, the point of zero flow. Curvature is relatively large when only K_2 is dependent on density *(top left* and *lower middle)*.

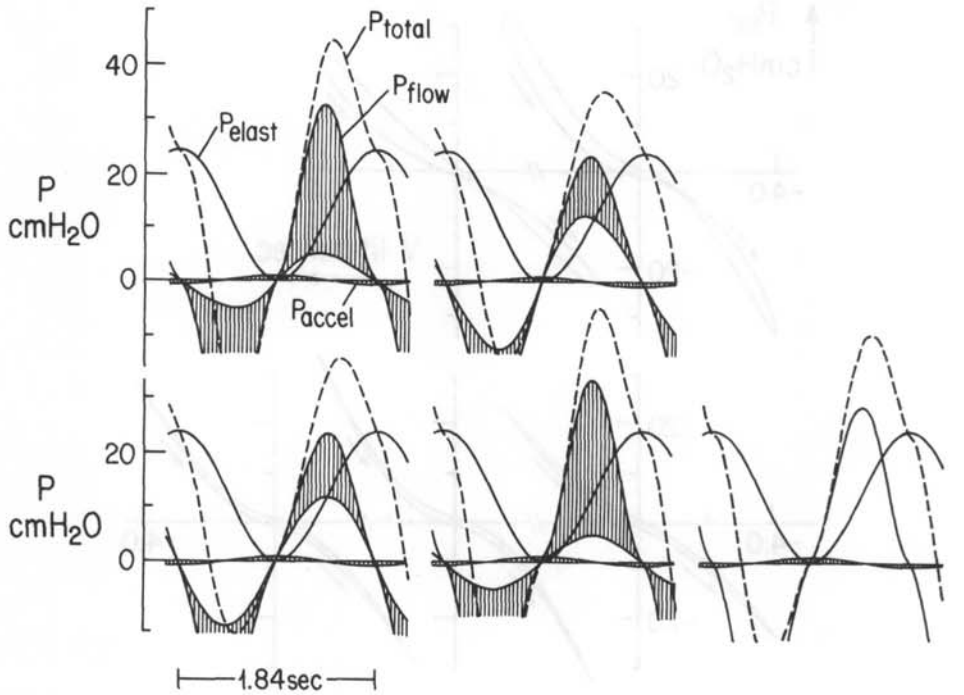

Fig. 4. Effects of alternative assumptions for the lung-volume and gas-density dependences of flow pressure. Simulations are for exercising men, RGD = 6, tidal volume = 2.43 liters at 0.54/s, as in Fig. 3. *Lower left* and *lower middle* figures have no volume dependence. *Upper left* (duplicate of the upper left panel of Fig. 3) and *lower middle*, all density dependence in the K_2 term. *Upper middle* and *lower left*, density dependence is shared by K_1 and K_2. *Lower right*, both volume and density dependence implicit in the coefficient of flow. Equations for the upper left case were *1–11*, as in Figs. 1–3. Substitutions: *Upper middle*, Eq. *12* for Eqs. *8* and *11*; lower left, Eq. *13* for Eqs. *8–11*; lower middle, Eqs. *14* and *15* for Eqs. *8–11*; lower right, Eq. *16* for Eqs. *8–11*.

DISCUSSION

A simulation is merely a display of the assumptions on which it is based; simulations are of value if they help one to develop a perspective about the relationships between variables. Three issues that are clarified by the results above are especially noteworthy.

First, although pressure for volume acceleration was increased by high gas density and high respiratory frequency, accelerative pressure was never an important fraction of total pressure for breathing in these simulations. Accelerative pressure was dwarfed by the increase of flow pressure that occurs with high gas density or with the high flows that usually accompany high frequency. The cases shown in Fig. 2 indicate that P_{accel} does not become important, in the sense that it is at least as large as P_{elast}, until density and frequency are very high, beyond the realm of practical situations of exercise in hyperbaric environments. The dominant role of density in the pressure-to-flow relationship in dense-gas environments is illustrated well in Fig. 3: At 6 ATA *(upper left)*, the shaded P_{K_2} contribution (the assumed focus of density dependence)

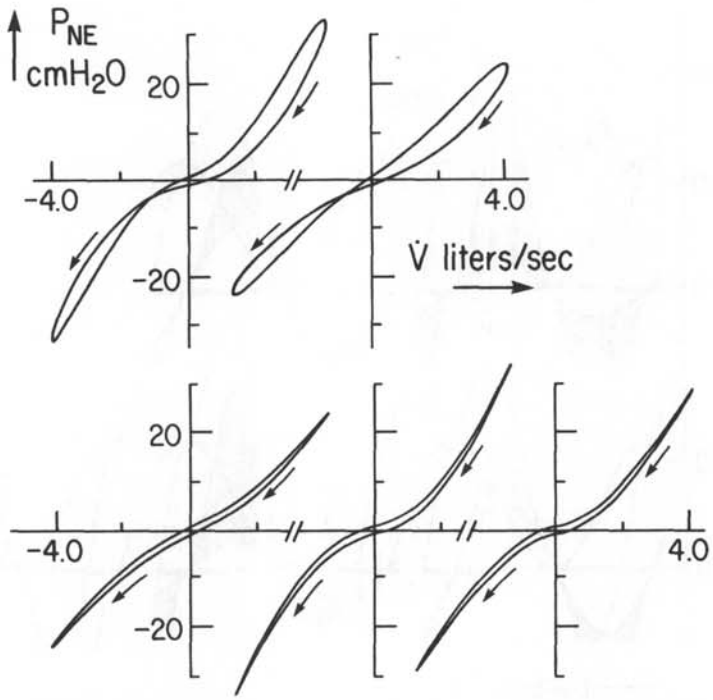

Fig. 5. Nonelastic pressure vs. flow; zero values for both are at the intersections of the axes. Patterns resulting from the same alternative assumptions as in Fig. 4 appear in the same order, *see* legend Fig. 4. *Small arrows* show time course.

exceeded P_{elast}, and peak P_{total} was about twice as large as peak P_{elast}. At normal density *(upper right quadrant),* PK_2 was approximately equal to PK_1 but P_{flow} was small compared to P_{elast}.

Most of the figures of this communication portray large, high-frequency breaths to emphasize the roles of P_{accel} and the density-dependent component of P_{flow}; these pressures would be less imposing with small tidal volumes at low frequency, where the low flows cause P_{flow} to be due mainly to PK_1, and total pressure would be dominated by elastic recoil. Figure 2, *lower left,* illustrates one case in which accelerative pressure is appreciable. In high-frequency breaths with very small tidal volumes in normal-density or low-density environments, flows could be low so that the PK_2 term of the Rohrer equation would not give rise to high pressures. This is not a practical issue with the large tidal volumes of exercise, but may be of interest in the context of high-frequency ventilation (21).

Although my simulations showed accelerative pressure to be small compared to flow pressure, the importance of acceleration in dense-gas environments cannot be considered a closed issue. My choice of a sine-wave function for volume vs. time yields slower second derivatives of volume with time than other patterns might, and it is uncertain how fast the change of direction of flow could be. If volume were a perfect ramp function of time, and inspiratory flow were constant until it jumped instantaneously to expiratory flow, acceleration would be indeterminate. In addition, there may be second-order accelerative phenomenon in dense-gas environments that my simulations for a simple, one-compartment model cannot account for, such as

change of the distribution of ventilation by enhancement of flow to lung regions that are served by straight paths in the airways (22) or production of relatively high peak pressures in the alveolar regions (23).

The second issue that the simulations bring into perspective is the nonlinear nature of pressure for flow. The ratio of flow pressure to flow fluctuates very markedly when P_{K_2} is an important element of the pressure for flow. Clearly, any idea of a certain unchanging airway resistance must be abandoned if the ratio changes from 2 to 8, as in Fig. 3.

Comparison of options

The third clarification provided by the simulations is that the different assumptions about pressure for flow have little effect on the pressures that are calculated. This is shown in the magnitude and timing of P_{total} (Fig. 4) and P_{NE} (Fig. 5). Inclusion of volume dependence made little difference to the patterns, but volume dependence could be an appreciable fraction of total pressures in normal environments where the P_{K_2} component is not so large.

It may seem surprising that the Maio-Farhi approach (Eq. *16*) and the Rohrer equation (Eqs. *8* and *12–14*) gave such similar results (compare *lower right* cases with others in Figs. 4 and 5). However, plots of pressure vs. flow derived from the two equations will superimpose within a few percent if the proper coefficients are entered into the calculations; it is a mathematical idiosyncracy that curvilinear data of the form of pressure-vs.-flow data can be characterized equally well by the sum of two terms, one with flow raised to the first power and one with flow raised to the second power, or by a single term with flow raised to a power between one and two (24).

The equation of motion is also an option, a deliberate choice of conceptual framework. The equation-of-motion framework makes the respiratory system analogous to an electrical system having capacitance, resistance, and inductance, and has been used with success in studies of impedance of the respiratory system (14–19); it has the advantage for present purposes that flow effects are by definition in phase with flow and accelerative effects are ½ cycle out of phase with volume. However, the framework has the weakness of the uncertainty about handling density-related changes in flow pressure, presumably caused by inertia of the gas, which I have explored here in use of Eqs. *5, 11–13, 15,* and *16*. Different frameworks are possible, as typified by the recent work of Isabey and Chang (25); through considerations of boundary-layer growth, inertial effects are taken to be integral to flow-pressure effects. This approach may prove to be a more realistic portrayal of the physical phenomenon, but it remains to be seen whether it improves conceptualization or predictive ability over the equation-of-motion approach.

The differences in patterns in Figs. 4 and 5 are so subtle that they would probably be within the errors encountered with experimental data. The Rohrer equation, the Eq. *16* option, and the assumptions about density dependence are simplifications, for application to intact man, of complex phenomena that probably are best studied in simple, well-controlled preparations or airway models (8, 25). The various assumptions can be considered equally valid; the investigators who used them simply characterized reality in different ways. Figures 1–3 have the advantage for didactic purposes that density and flow effects are manifested clearly in the one P_{K_2} term.

Inertance and natural frequency

Most measurements have yielded pulmonary inertance values close to the 0.01 $cmH_2O/(liter/s^2)$ used here, in human beings (1, 17), and in animals [dogs (15, 16, 18) and bonnet monkeys (19)]; three studies found inertance to increase in direct proportion to gas density (1–3). Kappos et al. (16) report data from open-chest dogs which allowed partition of impedance into components that were central and peripheral to a retrograde catheter in airways of 2-mm diameter; inertance could be completely accounted for by central airways, suggesting that tissue contributions to the inertance may be negligible. Frostell et al. (26) calculated an inertance that was 3.5 times greater than the value used here in a study of respiratory mechanics during a yogic practice, "quick short breathing"; trained practitioners took 350-ml tidal volumes at 230/min for 30–60 min. The high inertance value may be related to the steady-state nature of the yogic breathing or it may be due to technical aspects of the measurements. However, an inertance up to 5 times larger could have been used in the present simulations without making the P_{accel} an important fraction of P_{total}.

Even large increases in density will probably not decrease the natural frequency of the respiratory system enough to be in the range of frequencies expected in a working diver. The natural frequency can be expected to move from the normal 5 (27) to 1.7 and 1.2 cycles/s when density is 10 and 20 times normal (14). The high accelerative pressure that is brought on by high-frequency breathing or a dense environment has a minor effect on the phase relations between pressure, volume, and flow. Because the accelerative pressure counters elastic pressure, total pressure tends to be more nearly in phase with flow pressure than would otherwise be the case. For examples, consider the cases shown in Fig. 2. In the *top left panel*, if there were no accelerative component, P_{total} would have been moved slightly to the right; the effect would hardly be noticed because the large P_{flow} dominates the total pressure anyway. Even the right shift of P_{total} that would be caused by omitting P_{accel} from the *lower right panel* of Fig. 2 would be small because of the predominance of P_{flow} in the P_{total}.

Other issues

I purposely omitted several issues that could have made the simulations more realistic, but also more complex than needed to illustrate the points under consideration: a) Because of the omission of the nonlinearity of the pressure-volume characteristics of the respiratory system, peak P_{elast} values are underestimated, especially in Figs. 3–5, where tidal volume is large. b) Inertia of body structures, viscosity changes with density, tissue resistance, and laryngeal and nasal resistance were all assumed to be negligible. c) Flow dependence of airway dimensions gives rise to dynamic airway compression and flow limitation during forced exhalations; it has been argued that flow-limiting choke points constitute the ultimate limit to ventilation in dense-gas environments (28). The tendency for chokes to develop increases as density increases, and flow through choked airways is approximately inversely proportional to the square root of gas density (28, 29), so flow limitations could be anticipated in most of the dense-gas conditions simulated here. If so, the volume, flow, and pressure patterns during expiration are unrealistic in the direction that flows for given pressures would be less than those shown in the figures. The flow pressure-

to-flow ratio in a flow-limited airway is of the order of 15 $cmH_2O/(liter/s)$ in air at 6 ATA (20), double the maximal ratio shown in Fig. 3, lower right.

I am indebted to Dr. Barbara E. Shykoff for criticisms and encouragement.—*Manscript submitted July 1986, revision received December 1986.*

Van Liew HD. Composantes de la pression requise pour respirer des gaz denses. Undersea Biomed Res 1987; 14(3):263–276.—Afin d'élucider l'impact de la haute densité des gaz sur le débit des voies respiratoires (durant l'inspiration et l'expiration) et sur l'accélération des gaz (en fin d'inspiration et fin d'expiration), les pressions nécessaires pour respirer chez l'humain furent simulées avec: a) une équation de déplacement du système respiratoire, b) la supposition que la pression pour accélérer un gaz est proportionnelle à la densité, et c) cinq suppositions différentes concernant les relations entre le volume pulmonaire, la densité et la pression pour le débit. Les résultats montrent que la pression accélératrice n'est pas une fraction importante de la pression totale avec les densités, volumes courants, et fréquences possibles lorsqu'il est supposé que le volume pulmonaire change comme une fonction de temps sinusale. L'effet mineur exercé par la pression accélératrice élevée est de tendre à faire entrer la pression intrapleurale en phase avec le débit, comme c'est le cas avec la haute résistance au débit. Les hypothèses alternatives concernant la pression pour produire un débit aboutirent en de petits changements dans les formes de la pression avec le temps, mais n'eurent pratiquement pas d'effet sur l'ensemble général. Comme conclusions: les effets du volume pulmonaire et de la densité sur la pression de débit peuvent être caractérisés avec succès de plusieurs façons, et le grand effet de la densité sur la pression de débit domine les besoins en énergie pour respirer dans les milieux gazeux de hautes densités.

voies respiratoires
résistance dépendante de la densité
recul élastique
densité d'un gaz
hyperbare
fréquence naturelle du système respiratoire
résistance pulmonaire
fréquence de résonnance
équation Rohrer
résistance dépendante du volume
inertance

REFERENCES

1. Mead J. Measurement of inertia of the lungs at increased ambient pressures. J Appl Physiol 1956; 9:208–212.
2. Peterson RE, Wright WB. Pulmonary mechanical functions in man breathing dense gas mixtures at high ambient pressures—predictive Studies II. In: Lambertsen CJ, ed. Underwater physiology V. Proceedings of the fifth symposium on underwater physiology. Bethesda, MD: Federation of American Societies for Experimental Biology, 1976:67–77.
3. Sharp JT, Henry JP, Sweany SK, Meadows WR, Pietras RJ. Total respiratory inertance and its gas and tissue components in normal and obese men. J Clin Invest 1964; 43:503–509.
4. Mead J. Mechanical properties of lungs. Physiol Rev 1961; 41:281–330.
5. Rohrer F. Der Stroemungswiderstand in den menschlichen Atemwegen. Pfluegers Arch Physiol 1915; 162:225–259.
6. Maio DA, Farhi LE. Effect of gas density on mechanics of breathing. J Appl Physiol 1967; 23:687–693.
7. Hesser CM, Lind F. Role of airway resistance in the control of ventilation during exercise. Acta Physiol Scand 1984; 120:557–565.
8. Wood LDH, Engel LA, Griffin P, Despas P, Macklem PT. Effect of gas physical properties and flow on lower pulmonary resistance. J Appl Physiol 1976; 41:234–244.
9. Pedley TJ, Schroter RC, Sudlow MF. The prediction of pressure drop and variation of resistance within the human bronchial airways. Respir Physiol 1970; 9:387–405.
10. Wood LDH, Bryan AC. Exercise ventilatory mechanics at increased ambient pressure. J Appl Physiol 1978; 44:231–237.

11. Bouhuys A, Jonson B. Alveolar pressure, airflow rate, and lung inflation in man. J Appl Physiol 1967; 22:1086–1100.
12. Vincent NJ, Knudson R, Leith DE, Macklem PT, Mead J. Factors influencing pulmonary resistance. J Appl Physiol 1970; 29:236–243.
13. Goldstein D, Mead J. Total respiratory impedance immediately after panting. J Appl Physiol 1980; 48:1024–1028.
14. Van Liew HD. The electrical-respiratory analogy when gas density is high. Undersea Biomed Res 1987; 14(2): 149–160.
15. Jackson AC, Watson JW, Kotlikoff MI. Respiratory system, lung, and chest wall impedances in anesthetized dogs. J Appl Physiol 1984; 57:34–39.
16. Kappos AD, Rodarte JR, Lai-Fook SJ. Frequency dependence and partitioning of respiratory impedance in dogs. J Appl Physiol 1981; 51:621–629.
17. Michaelson ED, Grassman ED, Peters WR. Pulmonary mechanics by spectral analysis of forced random noise. J Clin Invest 1975; 56:1210–1230.
18. Tsai MJ, Pimmel RL, Stiff EJ, Bromberg PA, Hamlin RL. Respiratory parameter estimation using forced oscillatory impedance data. J Appl Physiol 1977; 43:322–330.
19. Wegner CD, Jackson AC, Berry JD, Gillespie JR. Dynamic respiratory mechanics in monkeys measured by forced oscillations. Respir Physiol 1984; 55:47–61.
20. Hesser CM, Linnarsson D, Fagraeus L. Pulmonary mechanics and work of breathing at maximal ventilation and raised air pressure. J Appl Physiol 1981; 50:747–753.
21. Chang HK. Mechanisms of gas transport during ventilation by high-frequency oscillation. J Appl Physiol 1984; 56:553–563.
22. Clarke JR, Jaeger MJ, Zumrick JL, O'Bryan R, Spaur WH. Respiratory resistance from 1 to 46 ATA measured with the interrupter technique. J Appl Physiol 1982; 52:549–555.
23. Fredberg JJ, Keefe DH, Glass GM, Castile RG, Franz ID III. Alveolar pressure nonhomogeneity during small-amplitude high-frequency oscillation. J Appl Physiol 1984; 57:788–800.
24. Clarke JR, Fisher MA, Jaeger MJ. Inertance as a factor in uneven ventilation in diving. In: Bachrach AJ, Matzen MM, eds. Underwater physiology VII. Proceedings of the seventh symposium on underwater physiology. Bethesda, MD: Undersea Medical Society, Inc., 1981:225–233.
25. Isabey D, Chang HK. Steady and unsteady pressure-flow relationships in central airways. J Appl Physiol 1981; 51:1338–1348.
26. Frostell C, Pande JN, Hedenstierna G. Effects of high-frequency breathing on pulmonary ventilation and gas exchange. J Appl Physiol 1983: 55:1854–1861.
27. DuBois AB, Brody AW, Lewis DH, Burgess, BF Jr. Oscillation mechanics of lungs and chest in man. J Appl Physiol 1956; 8:587–594.
28. Van Liew HD. Mechanical and physical factors in lung function during work in dense environments. Undersea Biomed Res 1983; 10:255–264.
29. Hyatt RE. Expiratory flow limitation. J Appl Physiol 1983; 55:1–9.